

Supporting Information

Fused filament fabrication of PVDF films for piezoelectric sensing and energy harvesting applications

Rui Tao¹, Jiahao Shi², Mohammad Rafiee¹, Abdolhamid Akbarzadeh^{2,3} and Daniel Therriault^{1*}

¹ Laboratory for Multiscale Mechanics (LM²), Department of Mechanical Engineering, Research Center for High Performance Polymer and Composite Systems (CREPEC), Polytechnique Montreal, Montreal, QC, H3T 1J4, Canada

² AM³L Laboratory, Department of Bioresource Engineering, McGill University, QC, H9X 3V9, Canada

³ Department of Mechanical Engineering, McGill University, Montreal, QC, H3A 0C3, Canada

Corresponding Author

*daniel.therriault@polymtl.ca (D.T.)

Section S1. Photo of the poling setup.

Figure S1 shows the contact poling setup which consisted of three parts: an in-house-designed contact poling setup, a high voltage power supply (max voltage = 60 kV) and a hot plate. In the poling station, the positive high voltage cable from the high voltage power supply was connected to a copper rod with a diameter of 3 mm as the top electrode, and an aluminum plate was grounded as the bottom electrode. A ceramic-insulated resistance temperature detector (956-35110016, Mouser Electronics, Inc.) was mounted on the aluminum plate and connected to the hot plate to control the temperature of the silicone oil bath.

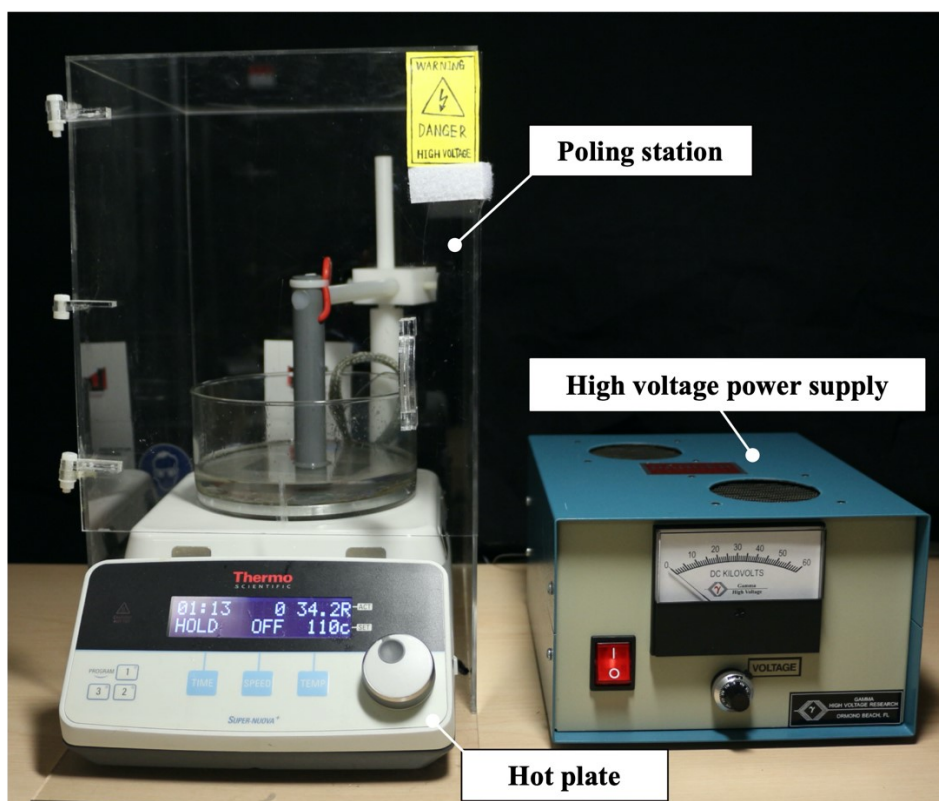


Figure S1. Photo of an in-house-designed contact poling station: a poling head (-), a silicone oil bath and an aluminum plate (+) (left) and a high voltage power supply (right).

Section S2. Optical images of the top surface of the well-printed PVDF film and the printed PVDF film with defects.

Defect-free printed PVDF films are important for the post-processing, i.e. stretching and poling processes. **Figure S2** shows the optical images of the well-printed (**Figure S2a**) and the printed PVDF films with defects (**Figure S2b**). As shown in **Figure S2b**, thinner section between the printed lines and the defects not only result in the failure during the stretching process but also limit the amplitude of the poling electric field during the poling process. In order to achieve a good printing without the thinner section between the printed lines, the printing bed should be well leveled and the extrusion width is decreased from 0.48 mm to 0.40 mm.

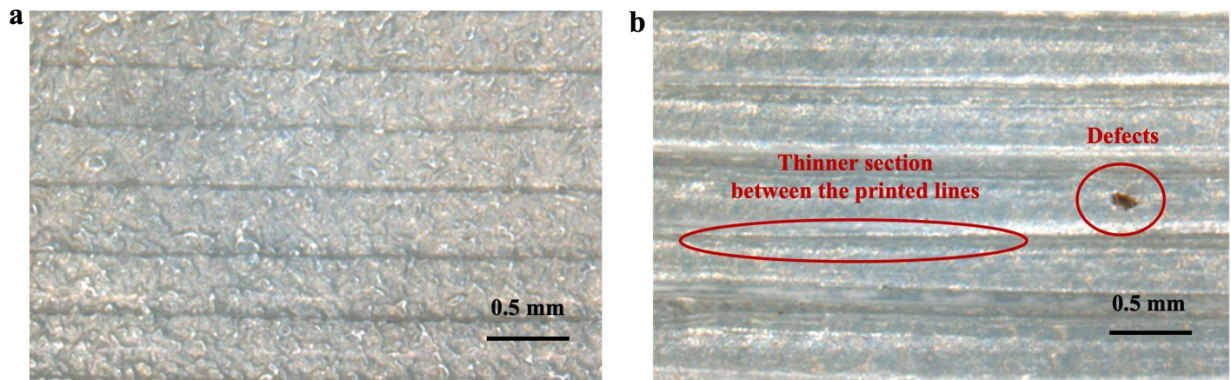


Figure S2. Optical images of the top surface of **(a)** the well-printed PVDF film, **(b)** the printed PVDF film with defects.

To quantify the thinner section volume fraction, we used a razor blade to cut a piece of sample (overall volume (V_0) = $10 \times 10 \times 0.15$ mm) from the well-printed and the with-defect FFF printed PVDF films, respectively. The density of the PVDF is 1.78 g/cm^3 . We measured their mass using a high-precision balance (GH-202, A&D Engineering Inc.) and computed the fully dense solid volume (V_s) by dividing the mass by the material density. The thinner section volume fraction is then calculated by:

$$\text{Thinner section volume fraction (\%)} = \frac{V_o - V_s}{V_o} \times 100 \quad (2)$$

The calculated thinner section volume fraction of the well-printed PVDF is $\sim 8.6 \pm 1.19 \%$, while the with-defect PVDF films is $\sim 28.0 \pm 1.78 \%$. Error bars indicate the standard deviation obtained from three replicates. The thinner section volume fraction of the well-printed PVDF films is reduced by $\sim 20\%$, which ensures the success of the poling process.

Section S3. Photo and thickness of the printed PVDF films with different R.

Figure S3 shows the photo of the stretched PVDF films at $R = 1, 2, 3$ and 4 . The thickness of the films were measured using a digital micrometer. The average thickness of the films and the poling voltage (i.e. electric field $30 \text{ V}/\mu\text{m}$) are listed in **Table S1**. Before the poling process, all types of PVDF films are cut into $40 \times 20 \text{ mm}$ from the center of the printed or stretched PVDF films.

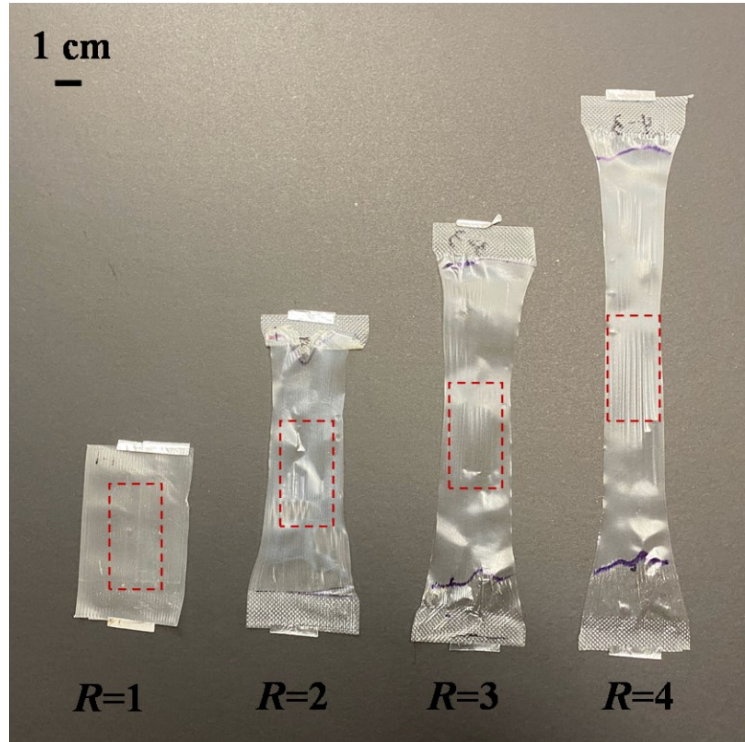


Figure S3. Photos of the stretched PVDF films at $R=1, 2, 3$ and 4 .

Table S1. Thickness of the stretched PVDF films.

R	Average thickness (μm)*	Poling voltage (kV)
1	153 ± 2.1	4.5
2	126 ± 2.5	3.6
3	92 ± 1.5	2.7
4	60 ± 1.2	1.8

*: Error bars indicate the standard deviations obtained from three replicates.

Section S4. Maximum allowable operating temperature for the printed polarized PVDF films.

To investigate the maximum working temperature of the piezoelectric PVDF films ($R = 4$; poling electric field = $30 \text{ V}/\mu\text{m}$) fabricated in this work, the polarized printed PVDF films were heated in the silicone oil bath at 30, 40, 50, 60, 70, 80, 90 and 100°C for 1 hr, respectively, and the piezoelectric coefficient (d_{33}) were measured by the d_{33} meter at three different locations before and after being heated (**Figure S4**). We find that the PVDF films start to lose its piezoelectric performance gradually when the temperature is above 60°C , which is consistent with the reported maximum operating temperature of commercial PVDF piezo sensors.⁵³ The reason is that the higher mobility of PVDF molecules at an elevated temperature results in the misalignment of the dipole moments. As a consequence, during the poling process, we need to cool down the piezo elements below 60°C before removing the poling electric field in order to avoid the misalignment of the dipole moments.

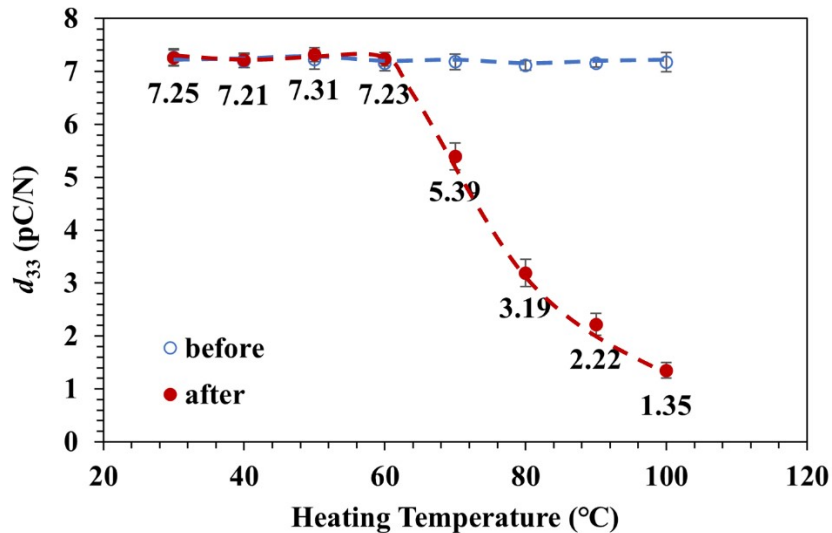


Figure S4. Piezoelectric coefficient d_{33} of printed polarized PVDF films before and after being heated at 30, 40, 50, 60, 70, 80, 90, and 100°C for 1 hr. Error bars indicate the standard deviations obtained from three replicates.

Section S5. Optimal voltage output and power output of the “piezo leaves” energy harvesters with the external resistance.

The effects of external resistance load on the voltage output of the “piezo leaves” are shown in **Figure S5a**. It can be observed that the voltage output increases with the external resistance. **Figure S5b** shows the instantaneous output power (P) at different external resistances (1 k Ω , 10 k Ω , 100 k Ω , 1 M Ω and 10 M Ω) calculated by:

$$P = \frac{U^2}{R} \quad (4)$$

where U is the output voltage and R is the external resistance as shown in **Figure S5a**. The maximum power output of the “piezo leaves” is ~ 0.45 μW when the optimum resistance is 1 M Ω . The instantaneous power density with the optimum resistance is calculated by:

$$S = \frac{P}{V} \quad (5)$$

where S is the power density and V is the volume of the four “piezo leaves”. The calculated S of the four “piezo leaves” is ~ 9.38 μWcm^{-3} at a resistance of 1 M Ω .

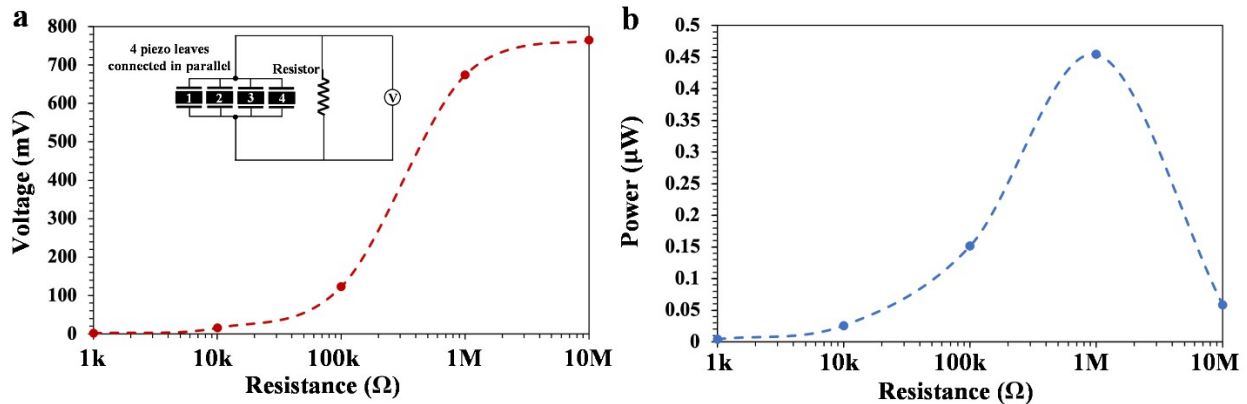


Figure S5. (a) Output voltage, (Inset: circuit diagram of the energy harvesting behavior test.) **(b)** Power of the “piezo leaves” with different resistances (1 k Ω , 10 k Ω , 100 k Ω , 1 M Ω and 10 M Ω) when the fan is turned on (1500 rpm).

Movies

Movie S1. Cantilever bending test: voltage output of the PVDF film sensors bent at 5 Hz and 10 Hz.

Movie S2. “Piezo leaves” energy harvesters: during a 3-min period of fan blowing (1500 rpm), the “piezo leaves” are able to charge the capacitor from 0 to ~ 2 V.